J Solid State Electrochem (2008) 12:569–574
DOI 10.1007/s10008-007-0398-x

ORIGINAL PAPER

Electrochemistry of platinum nanoparticles supported in polypyrrole (PPy)/C composite materials

Souad Mokrane · Laïd Makhloufi · Nicolas Alonso-Vante

Received: 10 January 2007 / Revised: 5 July 2007 / Accepted: 21 July 2007 / Published online: 6 September 2007

Abstract Conducting polypyrrole (PPy)/C (Vulcan XC-72) composite materials were synthesized by chemical polymerization method. These materials were used as matrix to support platinum nanoparticles, which were produced by the carbonyl chemical route. For the same catalyst loading (50 μg cm^{-2}), it was observed that the nature of the composite strongly influences the electrochemical activity of nanoparticulated platinum toward the oxygen reduction reaction in acid medium. The variation of the PPy/C ratio determines the so-called substrate effect for electrocatalysis.

Keywords Polypyrrole · Composites · Nanoparticles · Platinum-carbonyl · Substrate effect

Introduction

Intrinsic conducting polymers with conjugated double bonds have attracted much attention as advanced materials [1]. Among the electronic conducting polymers, polypyrrole (PPy) is especially promising for commercial applications because of its good environmental stability, facile synthesis, and high conductivity. PPy has been used as biosensor [2, 3], supercapacitor [4], electrochromic window display, packaging, polymeric battery, electronic device, and functional membrane [5, 6]. In electrocatalysis, PPy was recently used as a matrix for entrapping cobalt and generating active oxygen reduction reaction (ORR) sites [7]. PPy can be easily prepared by either an oxidative chemical [8–10] or electrochemical polymerization [11] of pyrrole. The long-term stability during cycling is a major demand for an industrial application of electronically conducting polymers (ECPs). Swelling and shrinkage of ECPs are well known and may lead to degradation of the electrode during cycling. This phenomenon occurs because the doping of polymers requires the insertion/deinsertion of counter ion, which causes a volume change. Thus, the mechanical stress in the polymer film relates directly with the life cycle of polymer-based capacitors for example. This has been overcome to some extent by the use of composite structures, i.e., a combination of ECPs and insulating polymers with good mechanical properties such as poly-*N*(vinyl alcohol) and polystyrene [12, 13]. However, in each case, the conductivity of the composite materials is lower than in the pristine form. Hence, the most interesting solution is to use carbon materials to improve the mechanical property of the electrodes. Moreover, the presence of carbon in the bulk of ECPs allows ensuring a good electronic conduction in the electrode when the polymer is in its insulating state. Electroconducting carbon additives generally provide a low specific capacitance in comparison to ECPs. Therefore, a compromise is necessary to minimize the carbon content in the composite to obtain a high value of specific capacitance.

Dedicated to Prof. Dr. Teresa Iwasita on the occasion of her 65th birthday in recognition of her numerous contributions to interfacial electrochemistry.

S. Mokrane · N. Alonso-Vante (✉)
Laboratory of Electrocatalysis, UMR-CNRS 6503,
University of Poitiers,
86022 Poitiers, Cedex, France
e-mail: nicolas.alonso.vante@univ-poitiers.fr

S. Mokrane · L. Makhloufi
Laboratoire Electrochimie et Corrosion,
Dépt. Génie des Procédés, University A. Mira,
Béjaïa 06000, Algeria

Experimental

Synthesis of polypyrrole–carbon composites

Five composites with different PPy/C ratios were synthesized according to the following protocol: Carbon dispersion was obtained by adding carbon (Vulcan XC-72 after heat treatment at 400 °C in air) and a volume of glacial acetic acid to a volume of ultra pure water Milli-Q Millipore System and stirring for 20 min at room temperature. Next, a mass of freshly distilled pyrrole (Merck, p.a.) was added to the carbon suspension and the stirring was continued for 5 more minutes, followed by the addition of a volume of an oxidant, $Fe_2(SO_4)_3$ solution (Labosi, p.a.). The mixture was stirred at room temperature for 4 h. The PPy-loaded carbon suspension was filtered, washed with water, and dried at 60 °C for 12 h. The resulting composites in powder form were characterized by elemental analysis, Fourier transform infrared (FTIR) spectroscopic, and thermogravimetric analysis (TGA). Table 1 summarizes the conditions for each PPy/C composite.

Physical-chemical characterization

C, H, N, and S elements were determined for PPy in composites by an elemental analyzer CE Instruments (NA 2100). FTIR spectra were recorded using a GX FTIR-Raman apparatus provided with a Nd:YAG laser. TGA were carried out in argon atmosphere at a heating rate of 10 °C min^{-1} up to 800 °C using a DSC-TGA SDT 2960 of TA Instrument. For the determination of catalyst particle size of samples, previously dispersed in methanol and placed onto a copper grid covered by a carbon film, an electronic microscope Philips CM120 equipped with a LaB_6 filament, was used.

Synthesis of Pt nanoparticles

Pt nanoparticles were prepared via the carbonyl chemical route, as reported in the literature [14, 15]. $Na_2PtCl_6.6H_2O$ (Alfa, 31.3% Pt) was dissolved in a solution of CH_3COONa (Labosi, p.a.) in methanol (Merck, p.a.). The solution, containing 2 mg Pt/ml, was stirred under carbon monoxide atmosphere (Air Liquid N47) at about 55 °C for 24 h with constant mechanical stirring until the solution turned green. This procedure led to platinum carbonyl complex formation $\left[Pt_3(CO)_6\right]_n^{2-}$, with n=6. Thereafter, 200 mg of finely crushed PPy/C was added to the platinum complex solution at room temperature under N_2 gas flow and stirred for more than 12 h to form the Pt/PPy/C composites. The solvent was removed and the filtrate subjected to heat treatment at 90 °C under hydrogen for 1 h. After annealing, the sample was washed with water until no chlorine ions were detected and then dried at about 60 °C. The dispersion of platinum nanoparticles is revealed by transmission electron microscopy (TEM). Figure 1 shows that small dark spots correspond to platinum nanoparticles distributed within the polymer framework. An analysis of the picture revealed an average size distribution of 1.89±0.49 nm of platinum.

Electrode preparation and electrochemical measurements

Pt/composite Nafion films were prepared from a suspension containing 2 mg of the powdered catalyst 20 wt%. Pt/composite, 0.1 ml of the solution of Nafion® (5 wt%, Aldrich), and 0.25 ml of ultra pure water from Milli-Q Millipore System (resistivity, 18.2 MΩ cm) were previously homogenized in an ultrasound bath for 1 h. A volume of 3 μl of this suspension was pipetted onto a mirror-finished glassy carbon (GC) surface disk electrode of 3 mm diameter. A catalyst loading of approximately 50 μg cm^{-2} was employed.

Electrochemical measurements were performed at 25 °C using an Autolab (type II) Potentiostat/Galvanostat. A conventional three-electrode electrochemical cell containing 0.5 M H_2SO_4 electrolyte out-gassed with nitrogen was used. A GC plate and a reference hydrogen electrode (RHE), connected to the cell through a Luggin capillary, served as counter and reference electrode, respectively. Before any electrochemical measurements and to eliminate any possible contamination from the Nafion®, the electrodes were activated by cycling at 50 mV s^{-1} between 0 and 1.2 V/RHE for Pt/PPy/C and between 0 and 1 V/RHE for Pt/PPy. This procedure allowed obtaining reproducible

Table 1 Chemical ingredients for PPy/C composite preparation and experimental-obtained PPy loading in each composite (last two columns)

PPy/C composites	Mass (g), carbon	Vol (ml), CH_3COOH	Vol (ml), water	Mass (g), pyrrole	Vol (ml), $Fe_2(SO_4)_3$	PPy (%)	Carbon (%)
17% PPy/C	2	0.5	15	0.4	24	11	89
33% PPy/C	1.6	0.4	12	0.8	48	28	72
50% PPy/C	1.2	0.3	9	1.2	72	35	65
67% PPy/C	0.8	0.2	6	1.6	96	50	50
83% PPy/C	0.4	0.1	3	2	120	62	38

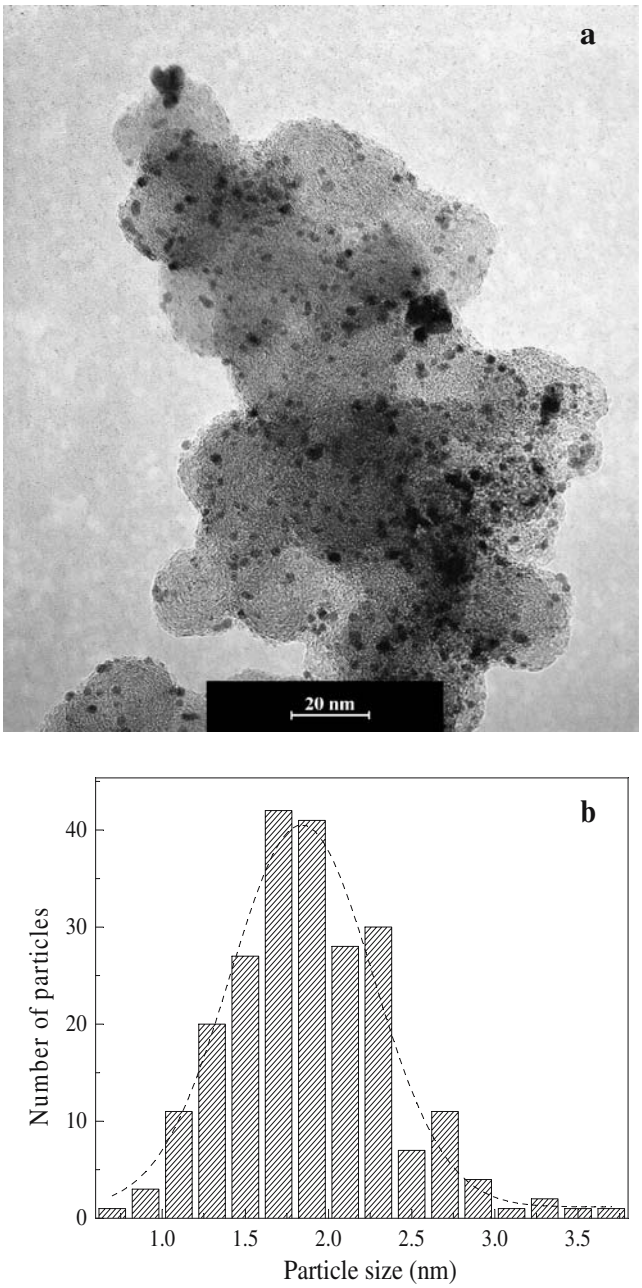

Fig. 1 **a** TEM image of 20 wt% Pt/PPy and **b** corresponding particle size distribution histogram

voltammograms. Surface-active platinum sites were probed with CO stripping measurements. For this, the experiment was carried out using pure CO, which was bubbled into the electrolyte for 5 min. The adsorption was made at a potential of 0.2 V/RHE for 3 min. Thereafter, the electrolyte was purged for 20 min with N_2 to eliminate CO dissolved in solution. The cathodic current of the ORR was recorded in an oxygen saturated 0.5 M H_2SO_4 solution under quasi-stationary conditions (voltammetric sweep at 2 mV s^{-1} between 1.0 and 0.0 V/RHE) for various angular scan rates, ω, from 0 to 3,600 rpm of the disc electrode using the rotating disk electrode (RDE) technique.

Results and discussions

Physical-chemical characterization

Elemental analysis The mass percentage determination of C, H, N, and S of PPy samples are 50.87, 3.60, 15.43, and 0.11%, respectively. Based on one nitrogen atom, the results correspond to the empirical formula, $C_{3.9}H_{3.3}N_{1.0}$, in agreement with the theoretical composition, $-(C_4H_3N_1)_n-$. A similar analysis was performed on carbon (Vulcan). As expected, C and H were found to be 95.62 and 0.22%, respectively. The 4.16% left can be attributed to the adsorbed impurities and oxygen species. The relationship between the experimental and theoretical values gives an average polymerization of about 75%; see last two columns of Table 1. The latter shows the real composition of PPy/C-composites.

Fourier infrared spectroscopy FTIR spectra, within an energy region of 400 to 2,000 cm^{-1}, of the prepared homopolymer (PPy), composites (PPy/C), and carbon (C) specimens are shown in Fig. 2. The main vibration modes of PPy were found to be the same as in previous works in the same conditions of synthesis [16, 17]. In short, for the homopolymer PPy, the frequencies at 1,698 and 1,559 cm^{-1} were assigned to the carbonyl group and to the C=C/C–C ring stretching of pyrrole. The bands at 1,472 and 1,290 cm^{-1} are due to the stretching vibration in the ring of C–N bond and C–H vibrations. The peak at 1,193 cm^{-1} is due to S=O stretching vibration of sulfonate anion. The peak at 1,098 cm^{-1} corresponds to deformation vibration of N H_2 on protonated nitrogen. The band of C–H and N–H in-plane deformation vibration of the pyrrole ring is situated

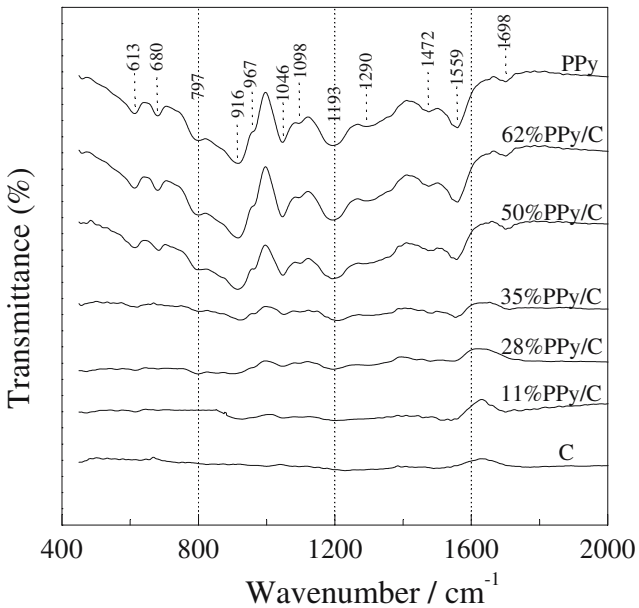

Fig. 2 FTIR spectra of polypyrrole (*PPy*) and PPy/C composites. Carbon is also shown for comparison

at 1,046 cm^{-1} and the band of the C–C out of plane ring deformation vibration at 967 cm^{-1}. The peaks at 916 and 797 cm^{-1} correspond to C–H out-of-plane deformation vibration of the ring and C–H out of plane ring deformation, respectively. Two more peaks at 680 and 613 cm^{-1} belong to C–H rocking and N–H out of plane vibration, respectively. The vibrational modes recorded on PPy emerge, within experimental error, at the same energy in the composite materials. No new bands or shifts were observed in the spectrum of PPy/C composites. This fact indicates a weak interaction of the polymer backbones with carbon (Vulcan). The intensities of the characteristic peaks were found to vary little in the composites containing 11 to 35 wt% PPy. However, such vibration modes emerge clearly at a PPy-loading higher than 35 wt%. Thus, one can summarize that PPy molecules are predominant in composites containing a loading ≥50wt%.

Thermogravimetric analysis TGA curves of the prepared homopolymer (PPy) and composite (PPy/C) specimens are shown up to 800 °C in Fig. 3. For comparison, the thermal stability of carbon (Vulcan) is also depicted in the same figure. All composite materials show a plateau between 100 and 200 °C after a weight loss of 6 to 9% mass, indicating that a similar process (i.e., residual humidity) is present in all composites and PPy. The weight losses of the samples in the range from 200 to 600 °C were observed to be about 5 to 29% mass going from 11 to 100% PPy. The thermal stability of PPy is affected in the composites materials, and the data suggest the overall thermal stability trends as follows: C>11% PPy>28% PPy>35% PPy>50% PPy>62% PPy>PPy. This trend appeared to be justified, as incorporation of more thermally stable C (Vulcan) particles into the less thermal stable PPy matrix led to the formation of composite with enhanced thermal stability compared to the homopolymer. The derivative of the weight loss with the temperature clearly shows a shift to higher temperatures from the less thermal stable homopolymer (PPy) to composites, see insert in Fig. 3.

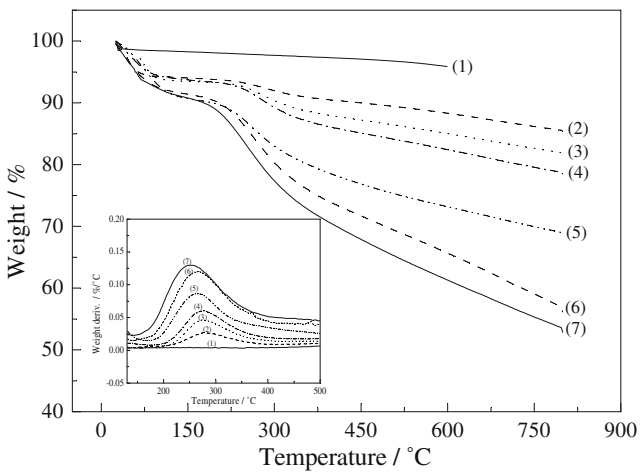

Fig. 3 TGA results at 10°C min^{-1}. *(1)* C, *(2)*11% PPy/C, *(3)* 28% PPy/C, *(4)* 35%PPy/C, *(5)* 50%PPy/C, *(6)* 62%PPy/C, and *(7)* PPy. *Insert* shows the weight derivative of the corresponding materials

Electrochemistry

Voltametric response Figure 4 contrasts the cyclic voltammograms of platinum nanoparticles embedded in various supports, namely, Pt/C, Pt/11%PPy/C, Pt/ 28% PPy/C, Pt/ 35% PPy/C, Pt/ 50% PPy/C, and Pt/PPy in nitrogen saturated 0.5 M H_2SO_4 at 25 °C at the scan rate of 50 mV s^{-1} between 0.05 and 1.2 V. To avoid irreversible oxidation of PPy, the potential interval for Pt/PPy electrode was scanned between 0 and 1.0 V. As expected, the electrochemical platinum fingerprint is found in the system Pt/C. The regions corresponding to adsorption and desorption of hydrogen, the double layer zone, and the water discharge and platinum surface oxidation/reduction processes are clearly defined. These characteristics are attenuated as far as the amount of PPy in the composite increases. However, one can still recognize such features up to a PPy loading of 28 wt% in the composite. At higher PPy loadings (>50%) in the PPy/C composites, the voltammetric response of platinum is dominated by the voltammetric response of PPy, cf. the system Pt/PPy in the figure. One interesting feature is the evolution of the double layer capacitance zone (0.3–0.42 V). In spite of the incorporation of platinum nanoparticles into the PPy/C composite for a loading higher than 50%, this zone becomes fully dominated by the PPy redox process: $PPy + SO_4^{2-} = [PPy^+SO_4^{2-}] + e^-$. In this process, PPy gets

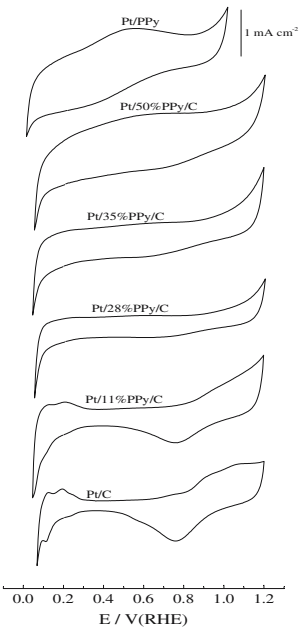

Fig. 4 Cyclic voltammograms in 0.5 M H_2SO_4 at 25 °C of Pt/C, Pt/PPy/C composites, and Pt/PPy with a scan rate of 50 mV s^{-1}

oxidized, and cation sites are produced thereby. The electroneutrality of the system is maintained through migration of SO_4^{2-} ions into the polymer matrix from the electrolyte. Similarly, during the cathodic sweep, anion sites are formed, and SO_4^{2-} are expelled from the matrix.

The probing of Pt nanoparticles' surfaces in the system depicted above was performed via stripping of CO monolayer previously adsorbed on Pt sites. Figure 5a shows this stripping process on Pt/C, Pt/11% PPy/C, Pt/35% PPy/C, and Pt/PPy recorded at 5 mV s^{-1} in 0.5 M H_2SO_4 electrolyte. The oxidation of CO on the Pt/C (Vulcan) system gives the highest peak at 0.8 V/RHE; the intensity of this peak decreases with the increase in PPy loading in the composite. However, besides this effect, we observe a concomitant shift to negative potentials of this stripping process. This shift, having a value of 20 mV for the system containing 35 wt% and of 120 mV in Pt, is only supported in PPy. This result is interesting because it shows that the electronic environment of Pt nanoparticles is strongly influenced by the presence of a conducting polymer, which is thermally, mechanically, and electronically stabilized by carbon in comparison to the PPy alone. Indeed, it is illustrative to mention that FTIR spectrum on Pt/PPy system (results not presented here) shows an energy red shift approximately 12 cm^{-1} of the vibration modes depicted in Fig. 2. This testifies the electronic interaction between Pt nanoparticles and the polymer backbones. The CO stripping experiments allowed for the determination of surface sites available for electrocatalysis. Taking into account that 1 cm^2 is equivalent to 420 μC [18], Fig. 5b shows the available platinum surface for each system. As expected, from data displayed in Fig. 4, the reduction of the platinum nanoparticles' surface is about 42% when the composite has a PPy loading of 28% in the composite.

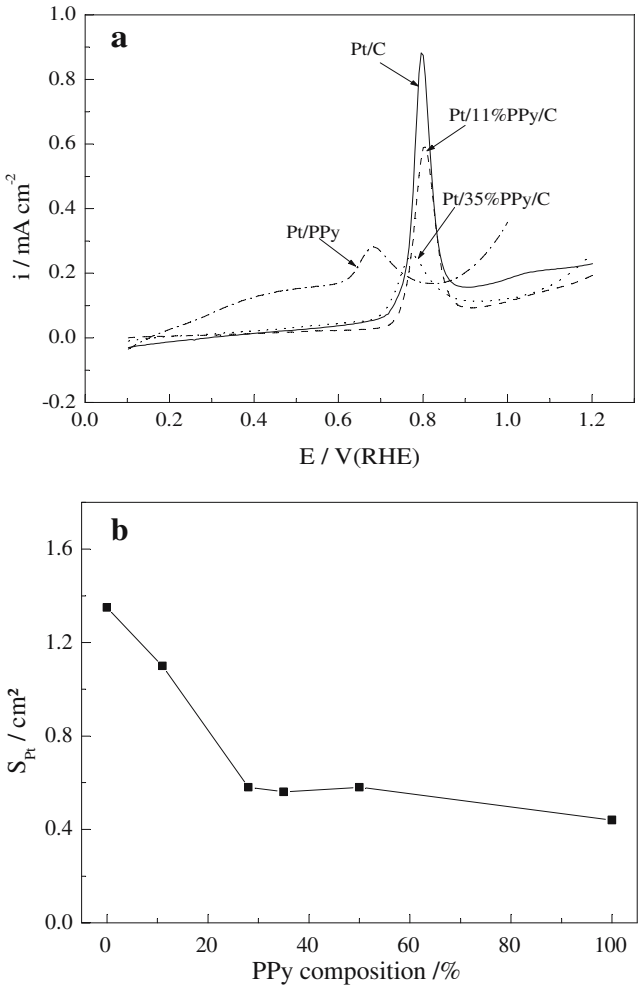

Fig. 5 **a** CO stripping in 0.5 M H_2SO_4 at 25 °C on Pt/C, Pt/PPy/C composites, and Pt/PPy; **b** platinum surface area (S_{pt}) as a function of the polypyrrole loading in composites with a scan rate 5 mV s^{-1}

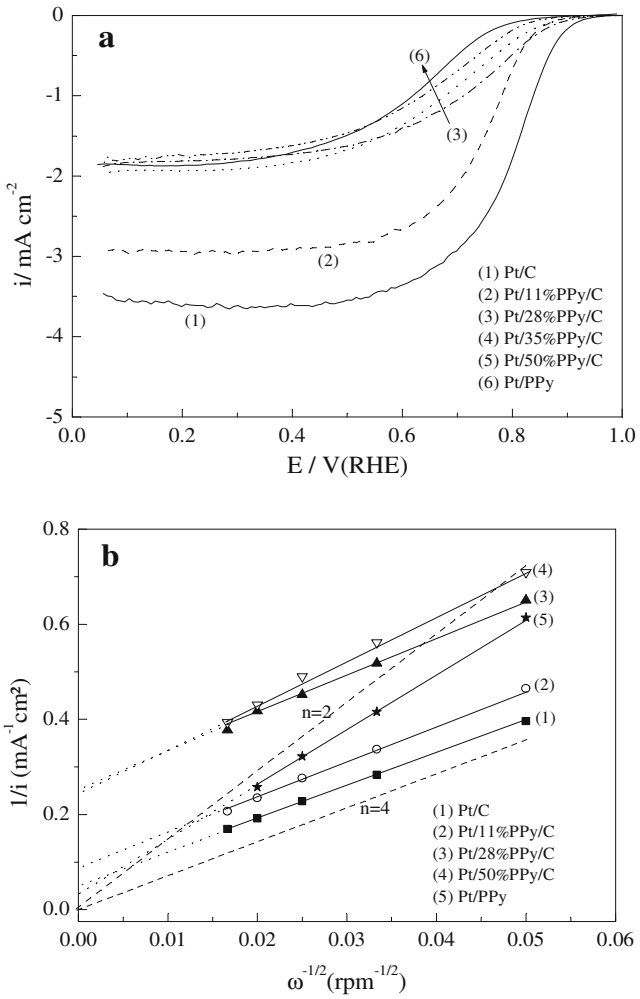

Fig. 6 **a** RDE current–potential curves of the oxygen reduction on Pt/C, Pt/PPy/C composites, and Pt/PPy deposited onto glassy carbon at 900 rpm, in 0.5 M H_2SO_4 at 2 mV s^{-1}, 25 °C. **b** Koutecky-Levich plots determined from ORR for Pt/C, Pt/PPy/C, and Pt/PPy composites at 0.10 V/RHE. The *dashed lines* refer to the two- and four-electron slope

Oxygen reduction reaction Figure 6 a shows a series of current-potential characteristics of the electrocatalytic oxygen reduction in 0.5 M H_2SO_4 on platinum supported on Vulcan, PPy/C composites, and PPy at 2 mV s^{-1} and 900 rpm. For all systems, the platinum loading was the same (50 μg cm^{-2}). As deduced by the CO-stripping measurements, a better electrocatalytic activity was recorded with the Pt/C system. Taking into consideration that the electrode thickness deposited onto GC disks of Pt/C or Pt/PPy/C, or Pt/PPy materials is the same, within experimental error, the observed limiting current densities have to be related to the available Pt sites in the PPy and/or PPy/C matrix. Indeed, the limiting currents for composites containing a mass of PPy>28% are approximately 50% of the value obtained with the Pt/C system. This result is in agreement with data generated via the CO-stripping process. To get an insight of the ORR electrocatalytic process and further influence of PPy, an analysis of RDE data was done. Figure 6b summarizes some selected Koutecky-Levich (K-L) plots for the ORR on Pt/C, composites Pt/PPy/C, and Pt/PPy. For the sake of clarity, only one straight line was drawn for each system at 0.10 V/RHE. First, for each system, all K-L plots showed straight lines, indicative of a first-order ORR. However, from the comparison among the systems, one observes that the slopes are somewhat different. Theoretical K-L slopes for $4e^-$ (water production), and $2e^-$ (hydrogen peroxide formation) were generated from the Koutecky-Levich (K-L) equation: $i^{-1} = i_k^{-1} + \left(B\omega^{1/2}\right)^{-1}$, where i_k corresponds to the kinetic current, $\left(B\omega^{1/2}\right)^{-1} = i_d^{-1} = (0.62\, n\, F\, A\, C^* D_{O_2}^{2/3} v^{-1/6} \omega^{-1/2})^{-1}$. B^{-1}, represents the K-L slope; n, number of exchanged electrons in the reaction, D_{O_2}, the oxygen diffusion coefficient; F, the Faraday constant; A, the electrode geometric area; v, the kinematic viscosity of the solution, and C^* the O_2 bulk concentration. Using a bulk O_2 solubility of 1.03×10^{-6} mol/cm^3, a diffusion coefficient of 2.1×10^{-5} cm^2/s and a kinematic viscosity of 1.75×10^{-2} cm^2/s in H_2SO_4 solution [19], the theoretical B values for four-electron and two-electron oxygen reduction were 7.76, and 15.53 mA^{-1} cm^2 $(rpm)^{1/2}$, respectively; see lines depicted in Fig. 6b. Based on these results, again, it appears that the presence of polymer backbones plays a major role in the mechanistic aspect of molecular oxygen reduction; as long as the PPy is present in the composite materials, the K-L plot shows that hydrogen peroxide production is being favored. Indeed, on the one hand, the electrochemical investigations on ECP-based electrodes in oxygen-saturated electrolytes indicated the existence of electrocatalytic activity toward the oxygen reduction [20, 21]. Oxygen reduction, in acid medium, takes place on PPy with an initial two-electron reduction of O_2 to H_2O_2 according to: $O_2+2H^++2e^- = H_2O_2 (E_0 = 0.682\ V)$. Similar observations were obtained on low platinum-loading (approximately 11 μg cm^{-2}) polyaniline [19].

Conclusion

Conducting PPy was synthesized in pyrrole/carbon to obtain PPy/C composite materials. The thermal and electrochemical stability of PPy was enhanced. This system served as support of Pt nanoparticles to study the ORR in acid medium. A substrate effect between metal nanoparticles and polymer backbones could be deduced at higher PPy content via the carbon monoxide stripping experiments. As a result, such phenomenon has an effect on the mechanism of the molecular oxygen reduction.

Acknowledgements SM thanks the financial support of the University of Béjaia, Algeria.

References

1. Gangopadhyay R, De A (2000) Chem Mater 12:608
2. Vidal JC, Garcia E, Castillo JR (1999) Anal Chim Acta 385:213
3. Ramanavicius A, Ramanaviciene A, Malinauskas A (2006) Electrochim Acta 51:6025
4. Conway BE (1999) Electrochemical supercapacitors. Kluwer, New York
5. Skotheim TA, Elsenbaumer R, Reynolds J (eds) (1998) Handbook of conducting polymers. Marcel Dekker, New York
6. Wallace GG, Spinks G, Teasdale PR (1997) Conductive electroactive polymers. Technomic, New York
7. Bashyam R, Zelenay P (2006) Nature 443:63
8. Omastova M, Pointeck J, Trchova M (2003) Synth Met 135–136:437
9. Kudoh Y, Akami K, Matsuya Y (1998) Synth Met 95:191
10. Jurevicinte I, Bruckenstein S (2003) J Solid State Electrochem 7:554
11. Mokrane S, Makhloufi L, Hammache H, Saidani B (2001) J Solid State Electrochem 5:339
12. Rubenstein E, Park JS (1991) J Appl Polym Sci 42:925
13. Campomanes RS, Bittencourt E, Gampos JSG (1999) Synth Met 102:1230
14. Longoni G, Chini P (1976) J Am Chem Soc 98:7225
15. Manzo-Robledo A, Boucher A-C, Pastor E, Alonso-Vante N (2002) Fuel Cells 2:109
16. Omastova M, Lazar M, Kosina S (1994) Polym Int 34:151
17. Furukawa Y, Tazawa S, Fujii Y, Harada I (1988) Synth Met 24:329
18. Ciureanu M, Wang H (1999) J Electrochem Soc 146:4031
19. Coutanceau C, Croissant MJ, Napporn T, Lamy C (2000) Electrochim Acta 46:579
20. Khomenko VG, Baruskov VZ, Katashinskii AS (2005) Electrochim Acta 50:1675
21. Singh RN, Lal B, Malviya M (2004) Electrochim Acta 49:4605